WIGGLE-MATCHED ^{14}C CHRONOLOGY OF EARLY BRONZE MEGIDDO AND THE SYNCHRONIZATION OF EGYPTIAN AND LEVANTINE CHRONOLOGIES

By Johanna Regev,[1] Israel Finkelstein,[2] Matthew J. Adams,[3] and Elisabetta Boaretto[4]
[Corresponding Author: Elisabetta Boaretto, Elisabetta.Boaretto@weizmann.ac.il]

Abstract

In a recent study by Regev *et al*. (2012), the radiocarbon data of Southern Levant was reanalyzed, causing a revision of the traditional absolute chronology of the Early Bronze Age in the Southern Levant. The new analysis demonstrated that the EB II was notably shorter than previously thought and that the EB III ended ca. 2500 BC, ca. 200–300 years earlier than the traditional chronologies. In order to understand how Megiddo fits into the new chronology, the authors designed and implemented a microstratigraphical excavation of the EB I to EB III strata at the site to identify new short-lived samples for radiocarbon dating. In modeling the results, we took advantage of known stratigraphical data to apply a wiggle-matching technique to the calibration curve, providing more precise dates for the samples. Overall, the dates from Megiddo are in line with the new radiocarbon-based chronology. These results as well as the implications of the dates for Egyptian-Levantine interactions of the 3rd Millennium BC are discussed.

Introduction

Megiddo is one of the most extensively excavated sites in Israel, and has enjoyed the status of type-site for the Early Bronze Age (EB) Southern Levant since the Oriental Institute (OI) excavations in the 1920s and 1930s (Loud 1948; Dunayevsky and Kempinski 1973; Esse 1991). While the relative stratigraphy and ceramic typology (relative chronology) of the site during that period is now well understood thanks to the renewed excavations by the Tel Aviv University-led Expedition in Area J (Finkelstein and Ussishkin 2000; Finkelstein, Ussishkin, and Peersman 2006; Adams 2013a; 2013b; Adams, Finkelstein, and Ussishkin 2014), its absolute chronology has not been sufficiently dealt with.[5] The traditional absolute dates for the EB layers at Megiddo depended on the relative regional chronologies established by the ceramic sequence, tied vaguely into historical dates of neighboring Egypt. Indeed, until recently such has traditionally been the basis for Early Bronze Age chronology for much of the Southern Levant. Unfortunately, few samples for radiocarbon dating were collected during the regular excavations in Area J, and thus there could be no independent, quantitative testing of the dates assigned to strata according to typological considerations.

A recent multi-site radiocarbon study of the Southern Levant in the EB (Regev, de Miroschedji, Boaretto 2012; Regev *et al*. 2012) has intro-

[1] Department of Land of Israel Studies and Archaeology, Bar-Ilan University, Ramat-Gan 52900, Israel; Weizmann Institute-Max Planck Center for Integrative Archaeology, D-REAMS Radiocarbon Laboratory, Weizmann Institute of Science 76100 Rehovot, Israel.

[2] Institute of Archaeology Tel Aviv University, Tel Aviv 69978.

[3] Jezreel Valley Regional Project, W.F. Albright Institute of Archaeological Research, 26 Salah ed-Din St., P.O. Box 19096, Jerusalem, Israel, 91190.

[4] Weizmann Institute-Max Planck Center for Integrative Archaeology, D-REAMS Radiocarbon Laboratory, Weizmann Institute of Science 76100 Rehovot, Israel.

[5] The renewed excavations at Megiddo are carried out by Tel Aviv University, with George Washington University as senior American partner. Consortium institutions are Chapman University, Loyola Marymount University, Vanderbilt University, University of Oklahoma, University of Hawai'i, and the Jezreel Valley Regional Project. The Expedition director is Israel Finkelstein (Tel Aviv University) with Eric H. Cline (George Washington University) serving as Associate Director (USA). Jennifer Peersmann supervised the excavation of Area J from 1996–2000 and Matthew J. Adams from 2004–2010. Radiocarbon analysis were supported by the Exilarch's Foundation and D-REAMS Radiocarbon Dating Laboratory.

Ägypten und Levante/Egypt and the Levant 24, 2014, 243–266

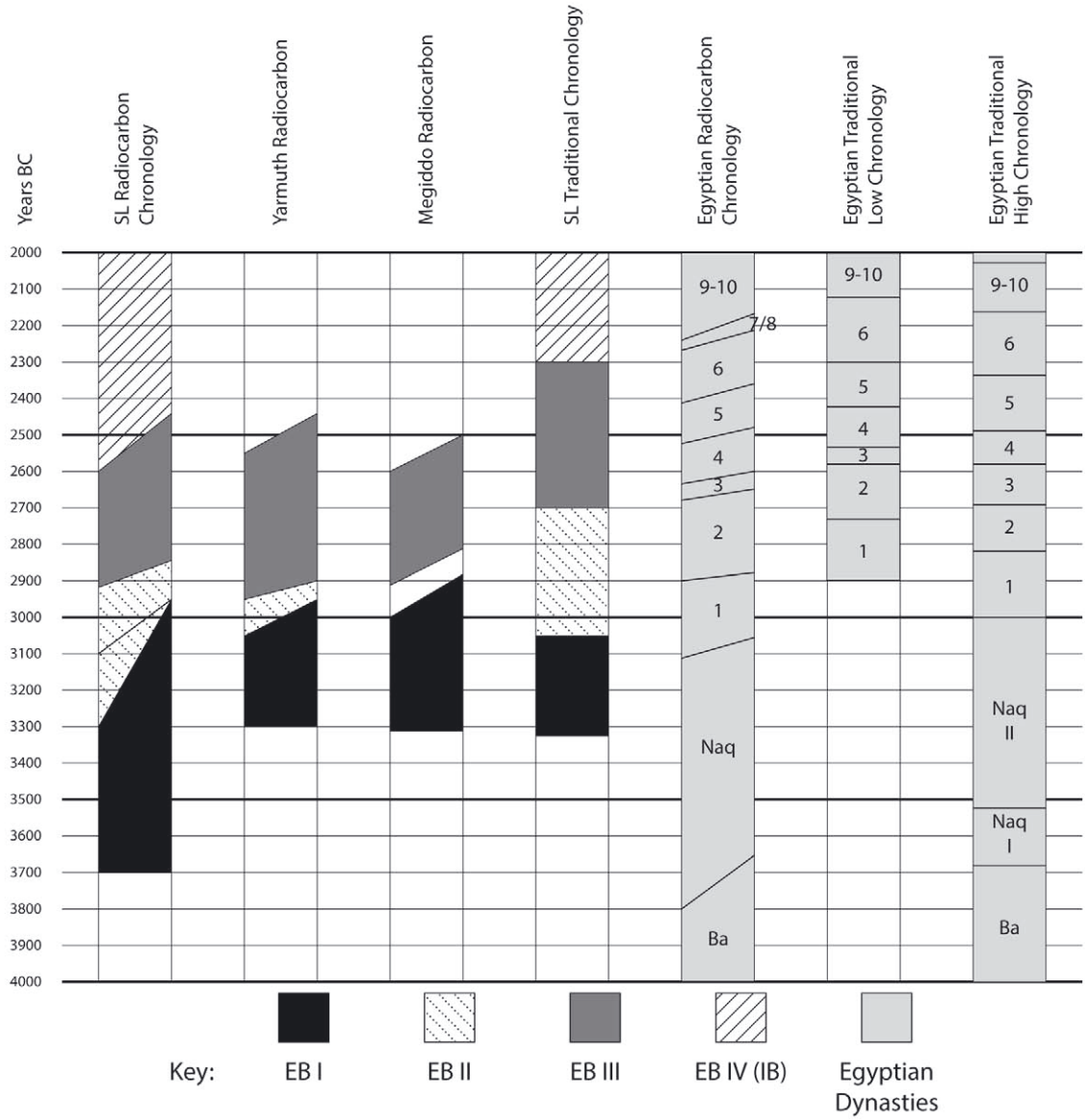

Fig. 1 Comparative chart of the Southern Levantine and Egyptian chronologies. The chronologies presented in the figure are based on the following reference from left to right: SL (Southern Levant) radiocarbon chronology (Regev et al. 2012), Yarmuth (Regev, de Miroschedji, and Boaretto 2012), Megiddo (this paper), conventional SL chronology (Mazar 1992), Egyptian radiocarbon chronology (Bronk-Ramsey et al. 2010, Dee et al. 2013), Egyptian traditional low chronology (Hornung et al. 2006), Egyptian traditional high chronology (Kitchen 1991). Within the radiocarbon chronologies the transitions between the periods are depicted as diagonal lines reflecting the range of time during which the transitions took place. In SL radiocarbon chronology the EB I to EB II transition appears very large, the single black line that appears in the middle of EB II transitional period depicts the EB I to EB II transition at the sites with the most robust data. For Megiddo, the EB II is not indicated in the figure, as no samples from this period were dated.

duced a radical new chronology in which the ends of EB II and EB III are placed ca. 2900/2850 and 2500 BC, respectively – 200 to 300 years earlier than the traditional chronology (Fig. 1). These findings have sparked a renewed interest in the absolute chronology of the period and its implications for internal cultural development and foreign interactions with Egypt, Syria, and further abroad.

As Megiddo is one of the best documented sites for this period, particularly in the northern sector of the region, it became imperative to synchronize it with other sites sampled within the context of the new radiocarbon chronology. Doing so would provide an important test-case for both the chronology and for the methods employed to attain it. This paper presents the results of a targeted micro-

Table 1: Summary of the Early Bronze Age Stratigraphy at Megiddo[6].

Level	*OI Stratum*	*Description*	*Period*
J-1	-XX, XX	Carved bedrock and associated structures	Chalc–EB I
J-2	Not detected	Temple and Picture Pavement	EB Ib
J-3	XIX	Temple 4050	EB Ib
J-4	XVIII	The Great Temple	EB Ib
J-4a	Not detected	Abandoned site. Sporadic squatter activity within The Great Temple	EB II
J-5	XVII	Palatial compound, streets and houses	EB III
J-6b	XVI	Palatial compound, streets and houses	EB III
J-6a	XVI	Palatial compound, streets and houses	EB III
J-7	XV	Temples 4040, 5192 and 5269	EB III (Finkelstein); Intermediate Bronze Age (Adams)

stratigraphic excavation through the sequence of Megiddo strata dating from the EB Ib through the late EB III (Levels J-4 through J-6a; Table 1) designed to recover samples for radiocarbon study, and discusses the dates of these samples within the context of the new radiocarbon chronology proposed by Regev *et al*. (2012). Further, the opportunity is taken to reconsider the overview of Egypto-Levantine interactions in the 3rd Millennium BC in light of this new chronology.

The Stratigraphy

The first stratigraphically identified occupation on the mound is evidenced by the bedrock hewing and poorly preserved elements of Level J-1 (Table 1), representing multiple phases of activity (Loud 1948: 59–63). The first clear discrete architectural phase, Level J-2, is defined by a cultic structure near the high point of the site (Finkelstein and Ussishkin 2000a: 38–55; Adams 2013a: Fig. 2.19), accessed from the eastern slope by way of a stone pavement. Ceramics from beneath this pavement secure its dating to the EB Ib (Adams 2013b). The structure was rebuilt in Level J-3 as a broad-room shrine (OI Temple 4050), a characteristic architectural style of EB I and EB II cult buildings, also dated ceramically to the EB Ib (Finkelstein and Ussishkin 2000a, 38–55; Adams 2013a, Fig. 2.20).

Later, but still within the EB Ib, the cultic landscape of the site was re-envisioned, and a massive new monumental temple (the Great Temple) was constructed (Level J-4; Figs. 2a–b; Adams 2013a; Adams, Finkelstein and Ussishkin 2014). This temple was abandoned at the end of the EB Ib and left to deteriorate through the EB II; during this period of slow ruination, it was occasionally visited by passersby or by people living in the vicinity, who were interested in perpetuating the cult within the ruins (Level J-4a).

The site was reoccupied at some point in the EB III (Level J-5; Fig. 3a), when a large palatial building was constructed on the eastern terrace (OI Building 3177; Loud 1948, 70–78, Figs. 392–393). This palatial compound was joined to a large urban space on the upper, western terrace, established on a thick brick-material fill covering the Level J-4 Great Temple (Adams 2013a: 82–94, 109–117). This palatial and urban architecture phase underwent at least two remodelings still within the EB III (Levels J-6b, J-6a; Figs. 3b–c). At the end of the Level J-6a phase, a dramatic reconfiguration of the site took place, in which the palatial and urban architecture was dismantled to make room for the construction of the three temples *in antis*, apparently of northern Levantine design, in Level J-7 (OI Temples 4040, 5192, 5269; Loud 1948: 78–84; Adams 2013a: 95–100, 117–118; Adams forthcoming). The relative dating of this phase is disputed, between the terminal EB III (Dunayevsky and Kempinksi 1973; Esse 1991; Finkelstein 2013: 1332–1333) and the Intermediate Bronze Age (Ussishkin 2013: 1324; Adams 2013a; forthcoming). In any event, by the Middle Bronze Age (OI Stratum XIV), the cultic area had been significantly reconfigured.

[6] As opposed to other areas where the current expedition operates, where the layers are numbered from top to bottom, in Area J they are numbered from bottom up; this is so because work here was undertaken in the area of the old excavations, with work beginning in the earliest monuments.

Fig. 2a Plan of the Great Temple of Level J-4 with 2012 excavated section marked.

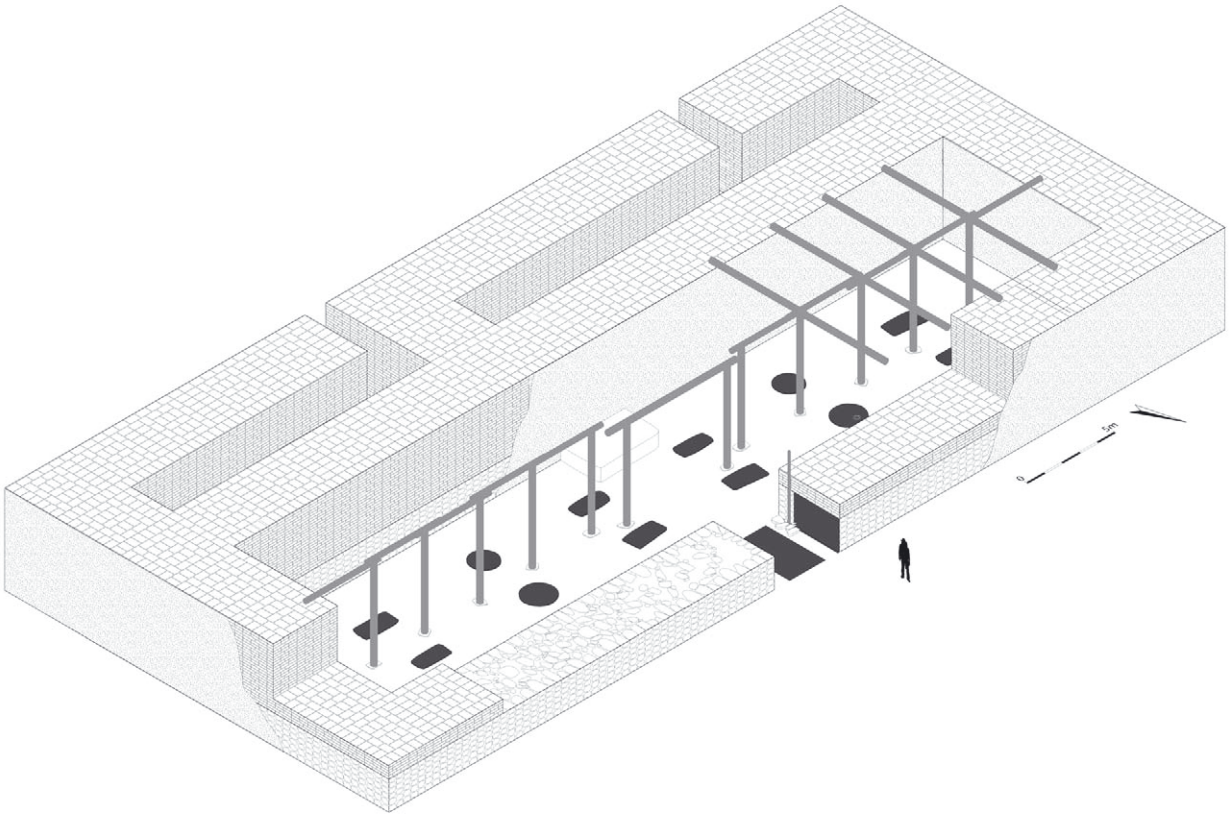

Fig. 2b Isometric reconstruction of the Great Temple of Level J-4.

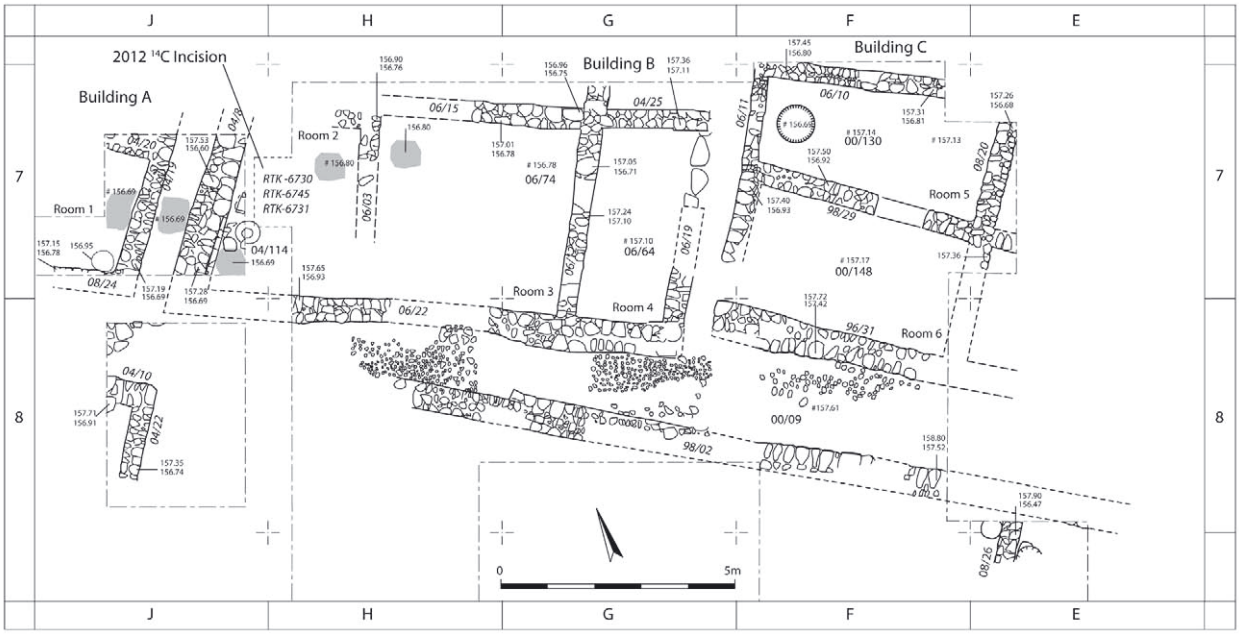

Fig. 3a Plan of Level J-5 with 2012 excavated section marked.

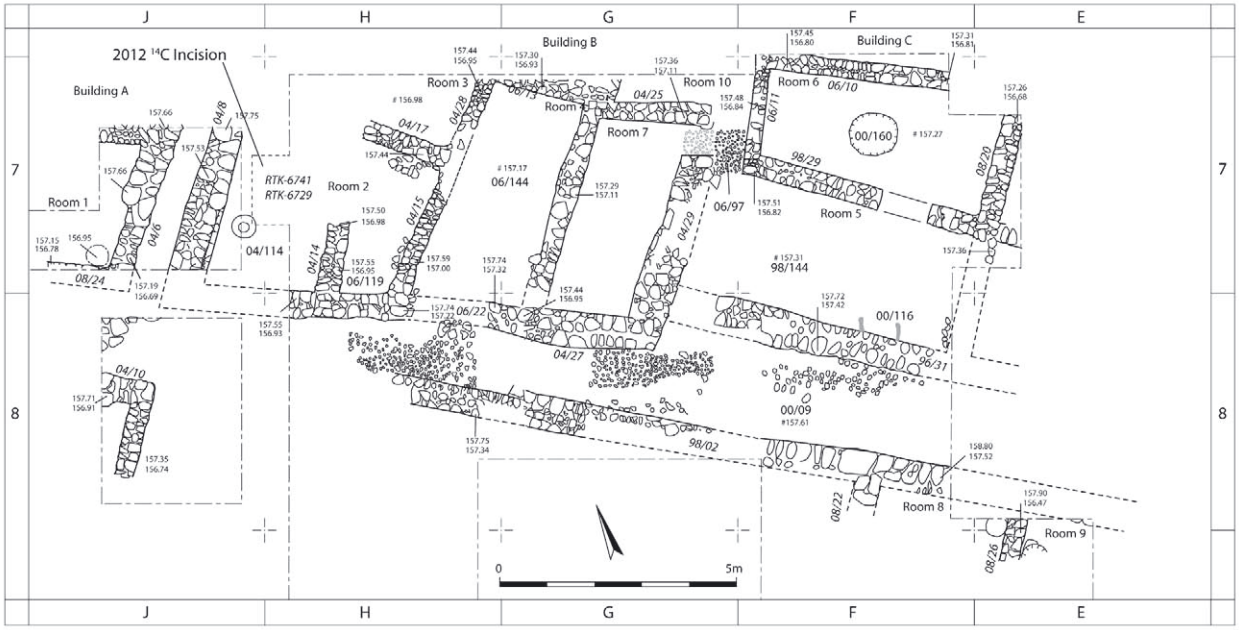

Fig. 3b Plan of Level J-6b with 2012 excavated section marked.

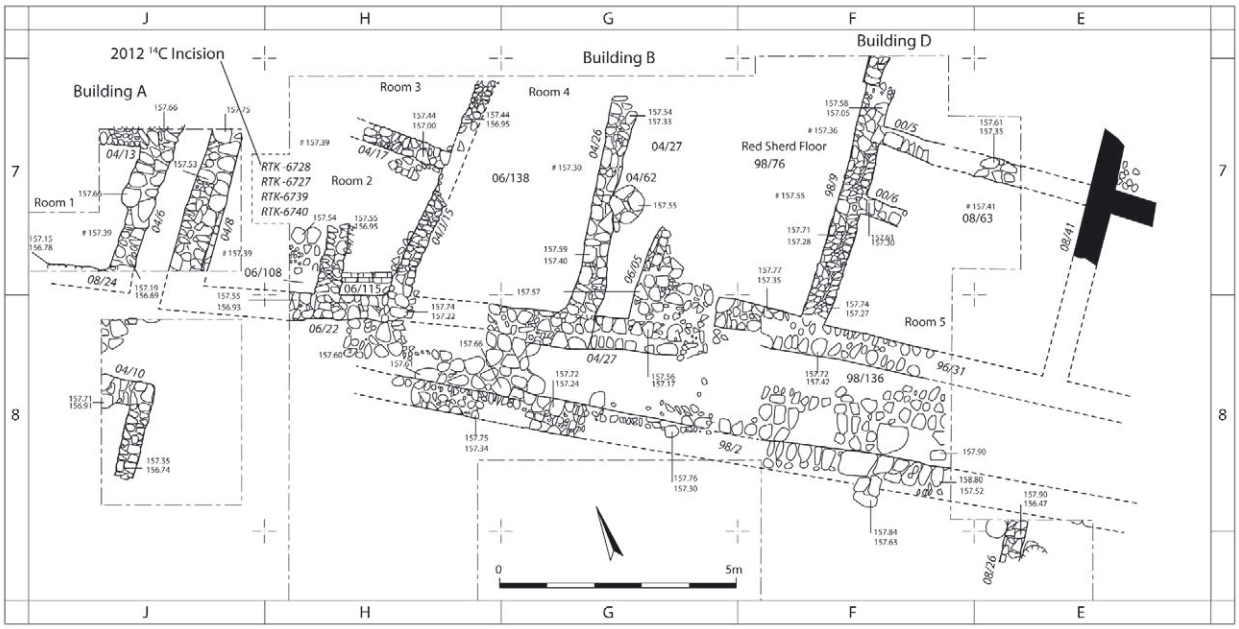

Fig. 3c Plan of Level J-6c with 2012 excavated section marked.

The 2012 Microstratigraphic ^{14}C Sampling Excavation

By the end of the 2010 season of excavations of the EB layers in Area J, five radiocarbon samples had been taken and dated, all originating from the EB Ib J-4 temple (Carmi and Segal 2000; Boaretto 2006). The three EB III levels (J-5, J-6b and J-6a) had not been sampled. We therefore designed a microstratigraphic excavation of a portion of the Area J EB sequence in order to collect new samples for ^{14}C dating. Since large-scale excavations in the area were completed in 2010, for our 2012 study we sought an exposed section adjacent to the recent excavations in the area. The criteria for this location included a well-understood stratigraphic sequence with clear floors for the layers in question, the presence of all phases from the late EB Ib through the EB III, and well-documented ceramic typology.

Fig. 4 Aerial photograph of Area J at the end of the 2008 season showing Level J-7 triple-temple complex (at surface), Level J-4 temple in deep squares, and location of 2012 microstratigraphical excavation marked in black rectangle. North is to the bottom of the photograph.

Fig. 5 Area J at the end of the 2008 season facing west. Location of 2012 microstratigraphical excavation marked in black rectangle.

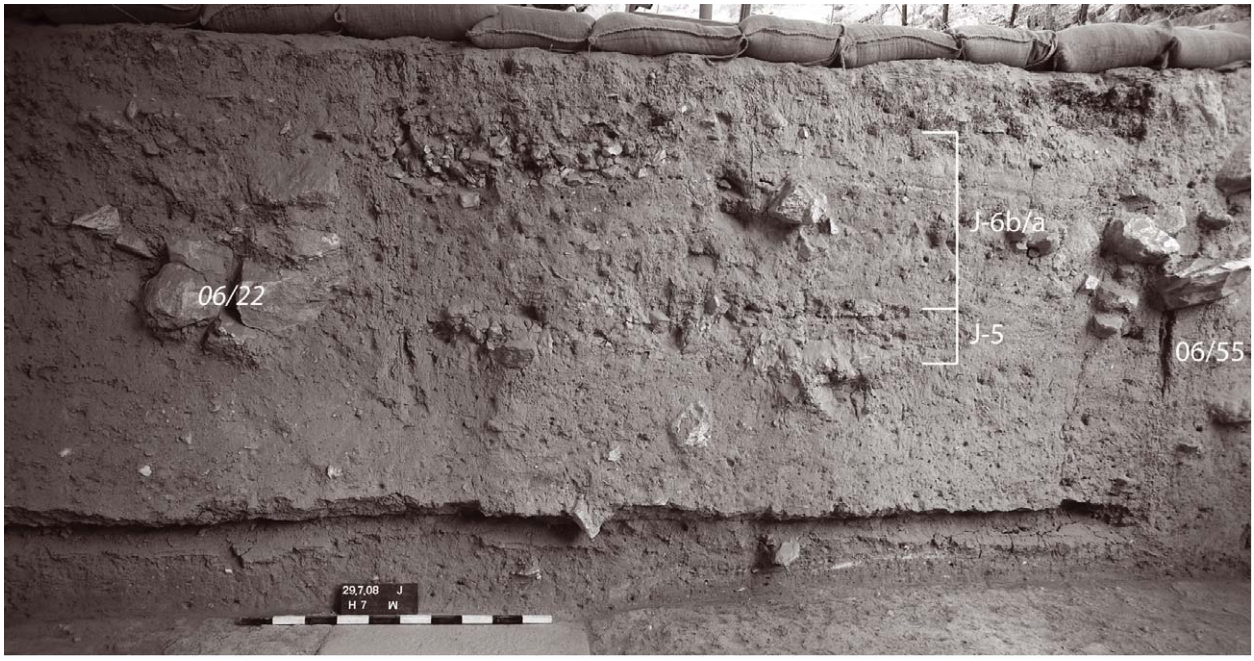

Fig. 6a Square H/7–8 west section indicating the EB III levels. Note Level J-4 basalt table (bottom left; below meter stick) and Phase J-4a accumulation broken by sinking of table (bottom center and right).

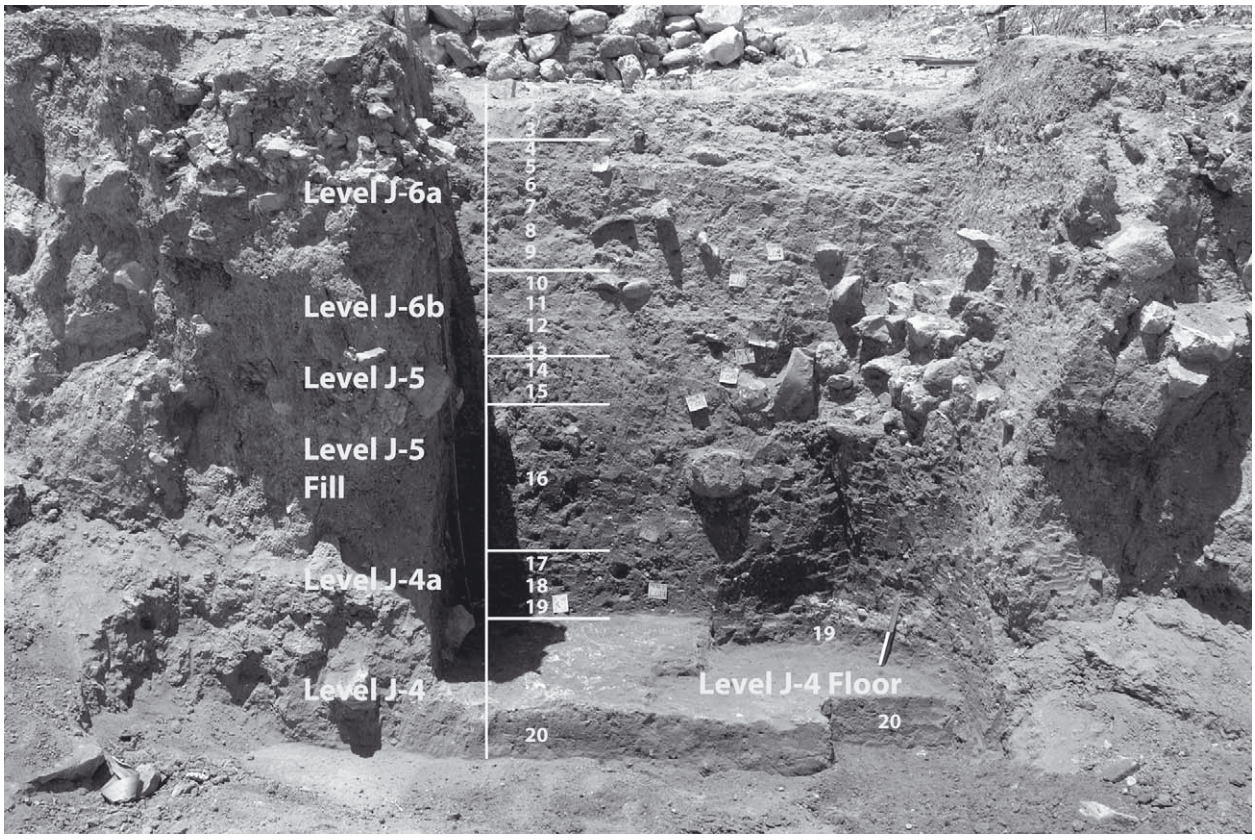

Fig. 6b Square H/7 west section after 2012 microstratigraphic excavation. Levels are marked at left and loci at right. Locus 21 does not appear in the figure, as it was excavated after the picture was taken. It consisted of 10 cm sediment below Locus 20. Level J-4 basalt table is beneath sediment in the far left of the photograph, at the level of the "Level J-4" label.

Table 2: Locus list and associated strata, height above sea level, archaeological context and mineralogy of the sediments associated with radiocarbon samples. The botanical identification is given with sample number. Legend: Cl=clay, (na)= non altered clay, (sa)=slightly altered clay,(a)=altered clay , C=calcite, (geo)=geogenic, not ash or plaster, CHAP= phosphates, opal=phytoliths

Locus	Stratum	Cultural Horizon	ASL (m)	Locus Description	FTIR Description of the Locus Sediment	FTIR Description of the ^{14}C Sample Context	^{14}C Sample	^{14}C Sample Context Notes
001				Erosional deposition since Chicago Excavations				
002			157.52-157.45	Phytolith rich, grey, friable sediment localized in SW corner of the unit	(altered 700°C) Cl (a)>C(geo),CHAP, opal.			
003			157.45-157.38	Hard, brown sediment, , perhaps mudbrick debris with EB III ceramic material in situ	Cl (na)>C(geo), little CHAP			
004	*J-6a*	EB III	157.39-157.38	Thin deposit below pottery (L.003) and above well-defined white surface (L.005)	Cl (na)>C(geo), little CHAP	(altered 600°C) Cl (a)>C (geo), CHAP, opal	RTK-6728 (cereal fragments)	Sample taken from a 20-cm diameter ashy lens rich in phytolith on a clear white surface (L.005). Stratigraphically, this sample may represent the very latest material belonging to J-6a or could possibly be a small hearth post-dating that phase.
005	*J-6a*	EB III	157. 38	0.5-cm-thick white surface identified only in the in eastern portion.	C (geo)>>Cl (na),	C(geo) >>Cl (na)*	RTK-6727 (Lens Culinaris)	Sample came from the matrix of the chalk surface. Seeds were found in the sifting of the matrix of the chalk
006	*J-6a*	EB III	157.38-157.27	Fill sediment, right below white surface (L.005). Consists of a mixture of greyish, friable sediment with seeds and hard brown sediments. In a small area, white friable material with seeds and in situ EB III pottery.	White sediment (a. 700/800°C) Cl (a)>>C(pyro), CHAP opal.	Greyish sediment (a. 400°C) Cl (sa)>C(geo), CHAP opal.	RTK-6739 (olive); RTK-6740 (olive)	Sample RTK- 6739 (L.006) was taken from west part from brown sediment, the same level as the white surface, but no white surface was identified above it. Sample RTK-6740was taken from 10 cm below the white surface (L.005) from ca. 20-cm-thick layer of phytolith rich, soft friable grey sediment.
007	*J-6a*	EB III	157.27-157.19	Friable grey, light brown, fill sediment with in situ pottery.				
008	*J-6a*	EB III	157.19-157.13	Brown sediment with a large fragment of an EBIII platter.				
009	*J-6a*	EB III	157.13-157.03	Brown, hard (mudbrick?) sediment and soft ashy material with many >10cm^3 stones and small sherds.				
010	*J-6b*	EB III	157.03-157.00	Light brown, hard pact sediment with a concentration of larger pieces of pottery and fragments of mudbrick(?)	Cl (na)>C (geo), little CHAP.	Cl (na)>C(geo) little CHAP	RTK-6741 (olive)	Lots of charcoal and some seeds were found among a concentration of potsherds

* According to FTIR (Regev et al. 2010; Chu et al. 2008), the surface was not plaster, but crushed local stone. Similar results came from other white surfaces and wall coatings at EB Megiddo (Friesem and Shahack-Gross 2013).

Locus	Stratum	Cultural Horizon	ASL (m)	Locus Description	FTIR Description of the Locus Sediment	FTIR Description of the ^{14}C Sample Context	^{14}C Sample	^{14}C Sample Context Notes
011	*J-6b*	EB III	157.00-156.90	Brown sediment giving way to a concentration of ash, phytolith and charcoal-rich light grey sediment and some lamination in the north.		C(geo) >Cl (sa) CHAP	RTK-6729 (olive)	Sample comes from a distinct sediment composed of ca.-2-cm-thick (40 cm in diameter) laminated ashy charcoal-rich deposit in the northern corner.
012	*J-6b*	EB III	156.90-156.87	Irregular laminated patches of ash, charcoal and seeds in the south with brown sediment in the north.				
013	*J-6b/J-5*	EB III	156.87-156.81	Cluster of 9 olive pits in brown mudbrick debris on an ash layer in the south.	Cl (na) =C(geo) little CHAP	Cl (na) =C(geo) little CHAP sediment nearby and below: (a. 700-800^{0}C) Cl (a)>C (ash) high CHAP,opal?	RTK-6730 (olive)	Sample originates from a cluster of about 9 olive pits found in brown unaltered sediment. Near and below the brown sediment, grey ashy sediment was identifiable, that could be connected to the origin of the olive pits. Based on previous excavation in the adjacent square, this sample could either be the latest deposit in Level J-5 or the earliest deposit in Level J-6b.
014	*J-5*	EB III	156.81-156.74	Brown sediment with 3 patches of grey ashy with charred material, two small stones concentrations, and an ash pit ca. 35 cm in diameter imbedded in brown sediment.	Cl (na)>C(chalk) little CHAP	(altered 700/800°C) Cl (a)>>C(?),CHAP, opal	RTK-6731, 6745 (Triticum aestivum compactum)	Samples measured came from the small ash lens consisting of phytoliths and seeds of various kinds. From a grain mount slide, several grass phytoliths were identified, in particular, from grass flowerlets, suggesting that wheat kernels could have been burned whole. Some ash pseudomorphs and dung spherulites were present. From sieving seven liters of this soft friable material, tens of seeds were recovered. The seeds were mainly wheat (*triticum aestivum compactum*), few wild species of *triticum*, some barley, and few wild species of barley, lentils (*lentisk culinaris*) and one grape pip. No olive pits were found. These samples represent the earliest EB III deposition.
015	*J-5*	EB III	156.81-156.74	Sediment around the L.014 ash pit, representing the matrix into which the pit sat. Brown sediments of mixed consistency surrounding L.014.				

Locus	Stratum	Cultural Horizon	ASL (m)	Locus Description	FTIR Description of the Locus Sediment	FTIR Description of the ^{14}C Sample Context	^{14}C Sample	^{14}C Sample Context Notes
016	fill		156.74-156.23	Very little pottery, charcoal or bones, mainly brown sediment.				
017	J-4a	EB Ib/ EBII	156.23-156.16	Brown sediment and fragments of white material. Lots of bones and sherds.				This level represents collapse of the J-4 temple (Level J-4a) as well as some of the brick fill which was laid over it in Level J-5. White material is collapsed from the chalk paste which originally coated the temple walls.
018	J-4a	EB Ib/ EBII	156.16-156.03	Brick debris mixed with white sediment. Lots of bones and charcoal.	White layer: C (geo)>>Cl (a) (500°C) reddish sediment in lump: (500°C) Cl (a)=C (lime), CHAP dark grey: Cl (na)>C (geo), low CHAP,			This level represents collapse of the J-4 temple (Level J-4a). White material is collapsed from the chalk paste which originally coated the temple walls.
019	J-4/J-4a	EB Ib/ EB II	156.03-156.01	This material is part of the J-4a collapse lots of bones, 2-3 layers of white material. Lots of charred material, but hardly any seeds. Burned bone.		C (chalk/ash)>> Cl (a)(altered 500°C), CHAP	RTK-6732 (olive)	This level represents collapse of the J-4 temple (Level J-4a). White material is collapsed from the chalk paste which originally coated the temple walls. In the lowest levels, below the earliest white chalk fragment a clear ash pocket was identified and 4 olive pits, one of which was dated. The sample represents deposit within the temple before the beginning of the collapse of the wall chalk. Therefore, the date of this sample provides a *terminus post quem* for the abandonment of the temple and a *terminus ante quem* for the construction of the temple.
020	J-4	EB Ib	156.01-155.90	Superimposition of a -cm-thick dark sediment, over a 2-cm reddish sediment, and thicker darker/ grey sediment.			RTK-6742 (Lens Culinaris)	Sample consists of a single lentil extracted from the reddish sediment, representing the constructional matrix of the Level J-4 temple floor, providing a *terminus post quem* for the construction of the Level J-4 temple.
021	J-4		155.90-155.80	Hard packed 5cm thick surface with lots of flint and some bone and pottery sherds. Below this is loose sediment with no charred material.				Constructional surface cut to prepare for the construction of the Level J-4 temple.

A section meeting these criteria was identified in the west baulk of Square H/7 (Figs. 2–6), which was known to contain the floor of the Level J-4 temple, an accumulation of debris from the collapse of the temple and activity therein (Level J-4a), and floors from the three phases of the EB III (J-5, J-6b, J-6a; Figs. 2–6). A 1.5 m × 0.75 m portion of the baulk was excavated to a depth of 2 meters to acquire the full sequence. This small excavation area proved advantageous in providing samples that were related to one another in a stratgraphic sequence without the often imprecise effort required in sampling across large areas. All strata excavated previously were identified after cleaning the section and marked prior to the beginning of excavation. A total of 21 contexts (loci) were excavated, representing the five levels, and 11 samples of the 130 taken were radiocarbon dated. The criteria for samples to be selected for dating were: a. short lived samples; b. seeds found in a cluster; c. associated with anthropogenic deposition (ceramics, ash, phytoliths etc.); and, d. of sufficient weight for analysis and of good preservation (enough material remains after pretreatment). Since no bones were found in articulation or in large concentration, only seeds were used for this analysis. Loci descriptions and the results of FTIR (Fourier Transform Infrared) analysis of the sediments for all the dated contexts are presented in Table 2.

Materials and Methods

Field Sampling Strategy for Radiocarbon Dating

Because the stratigraphy was well understood and the area of excavation limited, we were able to use a field sampling strategy that paid close attention to the microstratigraphy and focused on individual layers of sediment in a highly controlled manner. This strategy involved the following strategies:

a) Excavation was conducted mainly with small tools.
b) Sediment was removed carefully in thin (usually between 1–5 cm) layers using the visible vertical section as a guideline. As the type of sediment changed, or as special features were encountered, the locus number was changed, thus providing a unique number for each depositional layer.
c) Almost all charred remains were collected from each locus where encountered either in the field or from later dry sieving. Contexts were recorded with photos and detailed descriptions. Attention was paid to determine if the seeds collected could be considered a cluster or single dispersed items. All samples that were later chosen for ^{14}C dating were short-lived.
d) Sediment samples for FTIR analysis were systematically collected from loci which yielded ^{14}C samples and from the general matrix as control. These samples were analyzed for mineral composition and for the presence of anthropogenic features such as accumulation of ash, phytoliths, phosphate, burnt clay and plaster.
e) Artifacts (exclusively ceramics) were separated according to loci and compared with previously excavated assemblages.

Sediment Analysis and Botanical Identification of the Samples

Sediment samples were analyzed using FTIR Spectroscopy with a Nicolet 380 FTIR to identify different minerals and organic fraction. For several samples, grain mount slide analysis was performed.[7] There are several proxies used to identify anthropogenic sediments (Weiner 2010), depending on the type of activity that took place. The one used here is presence of phytolith, spherulites and pseudomorphs, levels of the phosphate mineral carbonated hydroxypatite (CHAP), indicating past presence of organic substances, temperature altered sediments (Berna *et al*. 2007), and grinding curve for calcite origin (Regev *et al*. 2010). In particular, in-situ ash or burnt deposits were detected using the proxies above. Prior to ^{14}C analysis, all seeds measured were botanically identified using binocular Leica M80.[8]

Pretreatment Towards Radiocarbon Dating

A total of 130 samples from 21 loci were collected in aluminum foil envelopes (each with several seeds or charcoal pieces in them). Context quality was

[7] Thanks to Shira Gur-Arieh (Kimmel Center of Archaeological Science, Weizmann Institute of Science and Land of Israel Studies and Archaeology, Bar Ilan University) for help with this.

[8] Thanks to Valentina Caracuta (Weizmann-Max Planck Center for Integrative Archaeology, D-REAMS Radiocarbon Laboratory, Weizmann Institute of Science) for help with this.

determined by microarchaeological methods (see above) and samples from the most secure contexts were selected for pre-treatment. In total 14 samples were considered for dating covering the whole stratigraphic sequence enabling high resolution modeling. The samples were pretreated for radiocarbon dating using the standard AAA (Acid, Alkaline, Acid) protocol (Yizhaq *et al*. 2005; Rebollo *et al*. 2008). It was necessary to repeat the alkaline treatment (NaOH 0.1N) once or twice for total removal of humic acids. The efficiency of the pretreatment varied greatly between samples, leaving between 5–55 % of the material at the end of the process. Combustion and oxidation to CO_2 was performed under vacuum at 900˚C with CuO. Once the CO_2 was obtained, it was transformed to graphite and pressed into cathodes. The ready cathodes were sent to the NSF-Arizona AMS (accelerator mass spectrometry) facility at the University of Arizona (Tucson, AZ) for ^{14}C determination. Only 11 samples were finally dated, as one sample tube broke during the oxidation process, for one sample not enough material was left after pretreatment, and in one sample a possible root was identified remaining after pretreatment. The samples selected with the information about context, species, and stratigraphic and cultural association are given in Table 2.

Radiocarbon Dating

The dating results are shown in Table 3. Radiocarbon ages are reported in conventional radiocarbon years BP (Before Present, where "present" is defined as year 1950) in accordance with international conventions (Stuiver and Polach 1977). Thus, all calculated ^{14}C ages have been corrected for the isotopic fractionation in order to be equivalent with the standard of δ^{13}C value of -25‰. The radiocarbon ages were calibrated using the OxCal 4.1.6 (Bronk Ramsey 2009) and the IntCal09 (Reimer 2009) calibration curve.

In addition to the samples collected in the 2012 microstratigraphic excavation, five samples from earlier excavation seasons had been previously dated, RT 2699, 2753 (charcoal; measured with decay counting method; Carmi and Segal 2000: 502–503) and RTT 3902–3903-3904 (olive pits; measured by AMS; Boaretto 2006). Since RT samples, measured by decay counting, were represented by several charred remains and are prone to old-wood affect, they were not considered in this study. Only the short-lived samples were added to the modeling in order to keep consistency with the new samples.

The calibrated ±1σ ranges of the EB III samples, even with the large 45–60 years uncertainties, all cover the period between 2890 BC and 2490 BC. The calibrated ±1σ ranges for EB IB samples are between 3090–2920 BC. Both are in agreement with the radiocarbon chronology results of the Southern Levant (Regev *et al*. 2012). However, it is possible to reach even more precise results and reduce the overlap between calibrated ranges by combining the stratigraphic information, radiocarbon dates, and calibration curve for the EB III in particular.

Models

The sequence of the new dates (labeled RTK) is shown in Figure 7, modeled according to stratigraphic sequence. Although the calibrated range is quite wide for several of the dates, by imposing the stratigraphic sequence on the model, three samples, RTK-6727, RTK-6729, and RTK-6731, can be considered outliers. They are, therefore, excluded from the following discussion; explanations for these outliers are given further below.

For the EB III, part of the overlap between the calibrated radiocarbon age ranges is due to the presence of wiggles in the calibration curve, which penalize the precision of the radiocarbon dates. By imposing the stratigraphic information and "wiggle matching" the dates with the stratigraphic sequence, it is possible to exclude part of the calibrated range for some of the dates.

Figure 8 shows the same ^{14}C sequence (as in Fig. 1) plotted on the calibration curve. If the dates from Loci 004 (RTK-6728), 010 (RTK-6741), 013 (RTK-6730) and 014 (RTK-6745) were plotted according to the radiocarbon age, without considering the wiggles in the calibration curve, a clear inconsistency between the stratigraphy and the radiocarbon dates would emerge. This inconsistence might have been explained by bioturbation of the sediments which was otherwise not detected in our microstratigraphic assessment. However, overlaying the samples with the calibration curve and maintaining the integrity of the stratigraphic sequence it is possible to increase the accuracy of the dates. In this model, some overlap of the calibrated ranges can be excluded or reduced since it is caused by the wiggle at 2900–2700 BC. It is important to reiterate that such reading of the dates is justified because their relative location is confirmed by the stratigraphic sequence. Moreover, if these results were obtained from samples

Table 3. Radiocarbon results for the samples measured in this study. For each sample the ^{14}C age, calibrated ranges and archaeological data are given. Pre 2012 samples are shown at the bottom of the table. The samples are ordered according to stratigraphy. The cultural period definitions cite the relative chronology of Levels J-5 through J-6a, and are not intended to imply ceramic or cultural divisions within the EB III (RT 2699 and RT 2753 are not included in the models presented here).

Sample number	^{14}C age ±1σ year BP	Calibrated range (BC) 68.2 % probability	Calibrated range (BC) 95.4 % probability	Locus	Stratum	Cultural Period
RTK-6728	4055± 45	2830 (5.0 %) 2820 2660 (2.3 %) 2650 2630 (38.9 %) 2550 2540 (22.0 %) 2490	2860 (10.3 %) 2810 2750(3.0 %) 2720 2700 (82.1 %) 2470	L. 004	Level J-6a	EB III late
RTK-6727	4375 ± 46	3080 (5.8 %) 3070 3030 (62.4 %) 2920	3310 (0.6 %) 3300 3285 (0.4 %) 3275 3270 (2.5 %) 3240 3110 (92.0 %) 2890	L. 005	Level J-6a	EB III late
RTK-6739	4125 ± 45	2860 (20.5 %) 2810 2760 (14.4 %) 2720 2710 (33.3 %) 2620	2870 (95.4 %) 2580	L. 006	Level J-6a	EB III late
RTK-6740	4125 ± 45	2860 (20.5 %) 2810 2760 (14.4 %) 2720 2710 (33.3 %) 2620	2870 (95.4 %) 2580	L. 006	Level J-6a	EB III late
RTK-6741	4200 ± 45	2890 (19.2 %) 2860 2810 (36.0 %) 2750 2730 (13.0 %) 2700	2900(27.1 %) 2830 2820 (65.8 %) 2660 2650 (2.4 %) 2630	L. 010	Level J-6b	EB III middle
RTK-6729	4010 ± 50	2580 (68.2 %) 2470	2840 (2.9 %) 2810 2680 (89.5 %) 2430 2420(1.2 %) 2400 2380 (1.8 %) 2350	L. 011	Level J-6b	EB III middle
RTK-6730	4120 ± 60	2860 (17.7 %) 2810 2760 (12.5 %) 2720 2710 (29.6 %) 2620 2610 (8.3 %) 2580	2880 (92.0 %) 2570 2520 (3.4 %) 2500	L.013	Level J-6b/J-5?	EB III middle/ early?
RTK-6745	4090 ± 55	2860 (14.3 %) 2810 2750 (6.0 %) 2730 2700 (45.5 %) 2570 2510 (2.4 %) 2500	2870 (19.3 %) 2800 2790 (0.7 %) 2790 2780 (65.9 %) 2550 2540 (9.5 %) 2490	L.014	Level J-5	EB III early
RTK-6731	3885± 45	2460 (60.8 %) 2340 2320 (7.4 %) 2310	2470 (86.9 %) 2270 2260 (8.5 %) 2210	L.014	Level J-5	EB III early
RTK-6732	4370 ± 45	3080 (1.5 %) 3070 3020 (66.7 %) 2920	3260 (1.6 %) 3250 3100 (93.8 %) 2890	L. 019	Level J-4a	Late EB Ib
RTK-6742	4400 ± 45	3090 (20.0 %) 3050 3040 (48.2 %) 2930	3330 (11.4 %) 3230 3220 (0.2 %) 3220 3170 (1.1 %) 3160 3120 (82.7 %) 2910	L. 020.	Level J-4	Late EB Ib
Samples from 1992–2000 excavations						
RT-2699	4500 ± 50	3340 (25.4 %) 3260 3240 (12.8 %) 3210 3200 (16.3 %) 3150 3140 (13.8 %) 3100	3360 (89.4 %) 3080 3070 (6.0 %) 3030	96/J/065/ LB008, (charcoal)	Level J-4	Late EB Ib
RTT-3904	4400 ± 40	3090(19.1 %) 3050 3030 (49.1 %) 2930	3320 (3.8 %) 3270 3270 (4.6 %) 3240 3170 (0.6 %) 3160 3120 (86.4 %) 2910	98/J/017/ LB020 (olive pit)	Level J-4	Late EB Ib

Sample number	^{14}C age ±1σ year BP	Calibrated range (BC) 68.2% probability	Calibrated range (BC) 95.4% probability	Locus	Stratum	Cultural Period
RTT-3903	4385 ± 45	3090 (9.8%) 3060 3030 (58.4%) 2920	3320 (2.6%) 3270 3270 (3.5%) 3240 3170 (0.3%) 3160 3110 (89.0%) 2900	98/J/065/ LB016 (olive pits)	Level J-4 and/or J-4a	Late EB Ib
RTT-3902	4365 ± 40	3020 (68.2%) 2920	3090 (95.4%) 2900	00/J/185/ LB015 (olive pits)	Level J-4	Late EB Ib
RT-2753	5030 ± 45	3940 (43.4%) 3860 3820 (24.8%) 3770	3950 (95.4%) 3710	Mixed debris in Temple 4050 (charcoal)	Level J-3	EB Ib

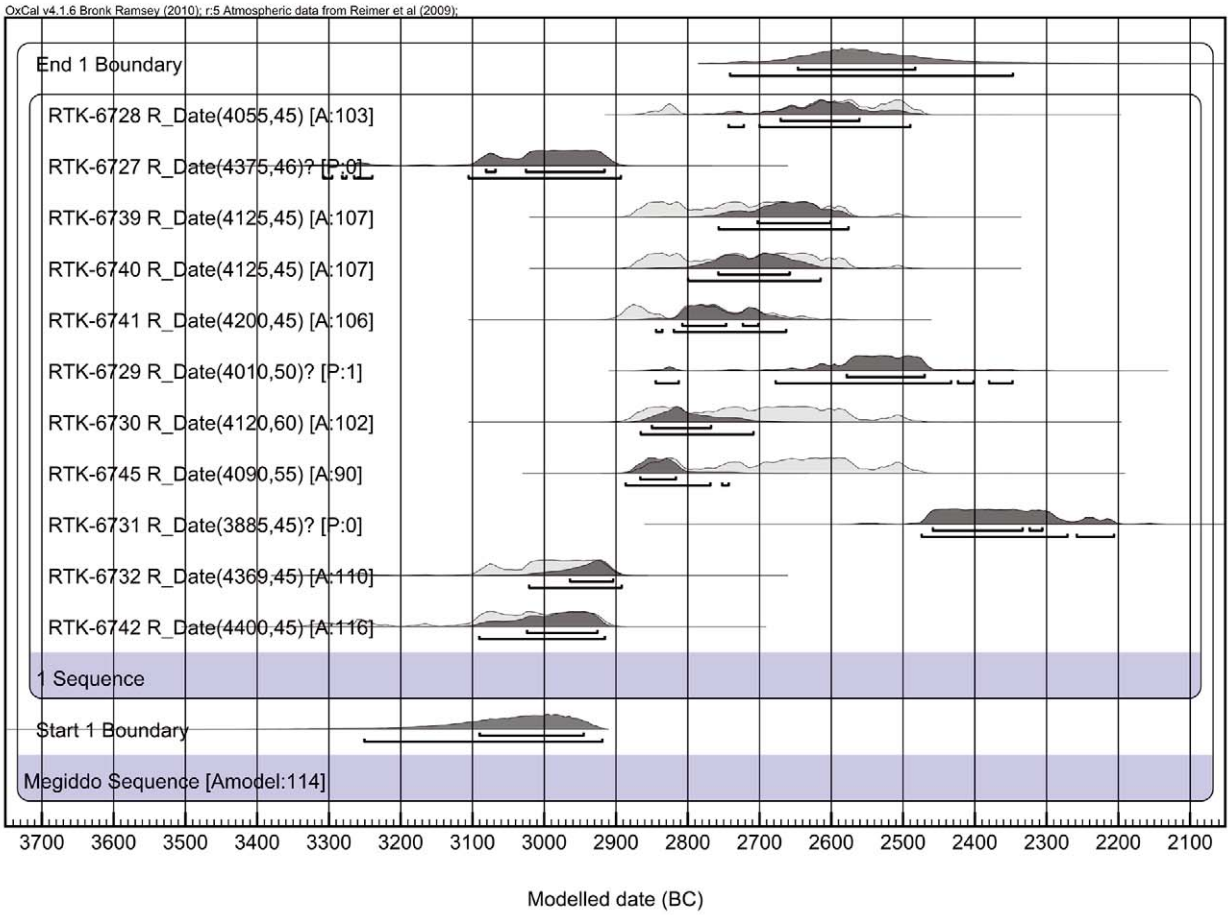

Fig. 7 The new Megiddo EB radiocarbon samples in modeled sequence according to height in the section and loci. The light grey plots depict the entire calibrated range of a single date, while the dark grey plots depict the modeled ranges. Outliers are marked with -?- and their entire ranges are colored only in dark grey.

collected from loci in different areas, without any stratigraphic relation, and based only on typology, the exclusion of part of the calibrated ranges would not be possible.

The wiggle matching of the dates versus stratigraphy places the earliest EB III occupation at Megiddo (Level J-5) between 2850–2800 BC. The middle EB III phase (Level J-6b) is placed between 2800–2700 BC, while the latest EB III sampled (Level J-6a) dates roughly to 2750/2700–2600/2500 BC. The calibration curve makes it possible to put this last phase (J-6a) on

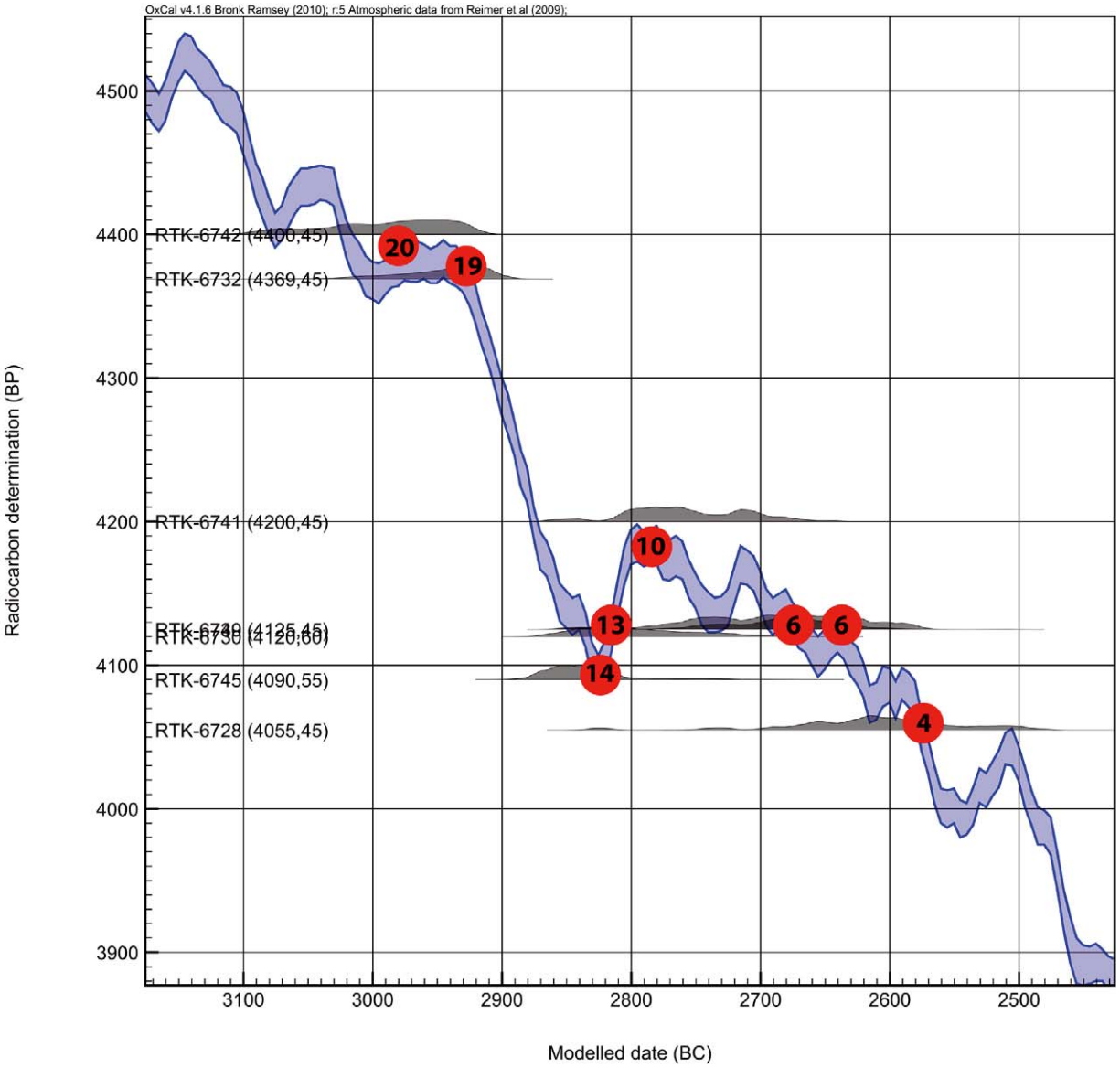

Fig. 8 Samples placed on the calibration curve according to the stratigraphic order of loci (in red) from which they were retrieved.

one of the wiggles in the 26th century BC (Fig. 8, Locus 004), albeit with a lower probability. As mentioned above, another possible (terminal) EB III layer (J-7; but see discussion of disagreement below) has not been sampled because all clean contexts had been removed by the Oriental Institute team.

The second model (Fig. 9; Table 3) was built as a sequence of sequences, meaning that the archaeological phases are ordered according to stratigraphy, and the samples within the archaeological phases are also ordered according to stratigraphy. In this model three short-lived samples taken from the Level J-4 temple (Boaretto 2006) were included (see Table 3; RTT-3902, RTT-3903 and RTT-3904). The outliers identified in the first model are also not included here. The boundaries of EB III sub-phases are contiguous since no gaps were identified between the archaeological phases. The boundary between the EB IB and the EB III is "sequential", since a gap in EB II exists between these two sequences (periods). The results are shown in Fig. 9 and Table 4.

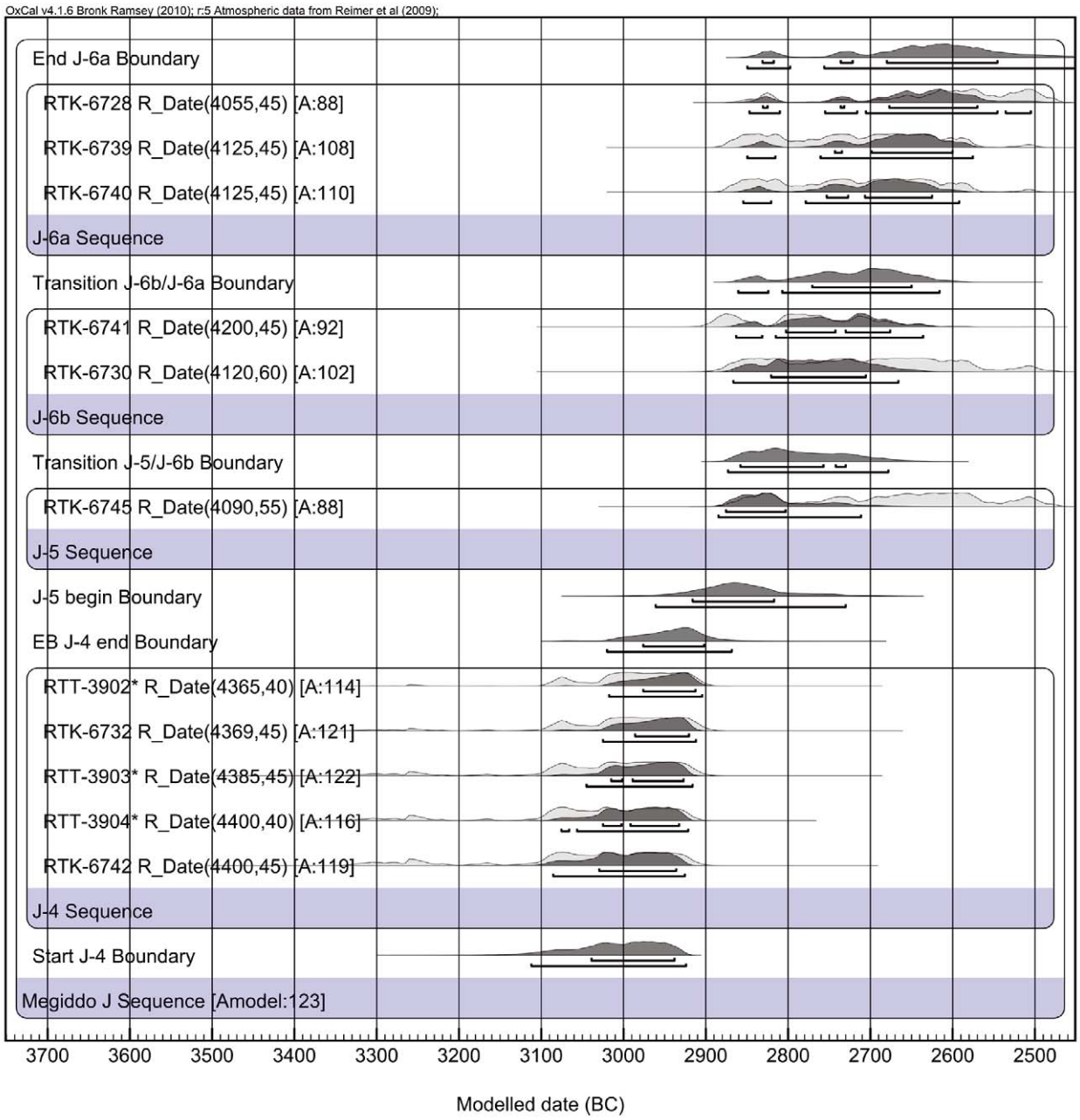

Fig. 9 Model based on the Megiddo Early Bronze levels, including the three previously published short-lived samples (Boaretto 2006). Outliers are excluded from this model. The model is built as a sequence of sequences, with contiguous boundaries between EB III layers, and sequential boundary between EB IB and EB III (see text for explanation).

Table 4. The calculated transitions for the various EB phases at Megiddo.

Boundary type	Stratum	Period	68.2% probability BC	95.4% probability BC
Start	J-4	EBIb	3060–2920	3180–2910
End	J-4	EBIb	2990–2880	3070–2830
Start	J-5	EBIII early	2920–2810	2970–2720
Transition	J-5/J-6b	EBIII early/ middle	2860–2720	2880–2670
Transition	J-6b/J-6a	EBIII middle/late	2770–2640	2870–2610
End	J-6a	EBIII late	2840–2540	2860–2450

The Outliers

Three outliers were identified during the modeling, all of them having below 60% agreement with the model. Sample RTK-6727 was collected by sieving the white surface of the latest EB III layer. The result was similar to RTK 6732 from Locus 19 taken from similar material from the J-4a layer above the temple floor. This sample might be best understood as residual material from earlier layers mixed into the white material/floor matrix. This date serves also as a reminder, that dates derived from construction materials are problematic, since it is difficult to tell their origin. In general, such dates can be used as a *terminus post quem* only.

Outlier RTK-6729 with the date 4010±50 ^{14}C year BP uncal is far too late for its stratigraphic association. This could be an intrusive sample or a laboratory outlier.

Outlier RTK-6731 comes from a small ash pit with lots of seeds in the earliest EB III phase (Level J-5). From the same context, two samples were dated: RTK 6745 and RTK 6731. While RTK 6745 agrees with the stratigraphic sequence, RTK 6731 (a single wheat grain), gave a date in 3885±45 ^{14}C year uncal BP – too late with respect to the other samples in the sequence. For this outlier, no explanation has been found.

Discussion

Figure 1 provides a comparison of the traditional relative chronology (Mazar 1992) and the new radiocarbon-based chronology of the Southern Levant based on Regev *et al*. 2012a, accompanied by data from a detailed study of Tel Yarmuth (Regev, de Miroschedji, and Boaretto 2012) and the new Megiddo radiocarbon data presented in this paper. These are shown together with new radiocarbon dates for Egyptian dynasties (Bronk Ramsey *et al*. 2010; Dee *et al* 2013) and traditional Egyptian dynastic chronologies (Kitchen 1991, Hornung *et al*. 2006). In the Southern Levantine radiocarbon chronology, the EB I to EB II transition appears very large (appearing in Fig. 1 as highly sloping transition line), either due to the lengthy transition period, lack of unity in the cultural definition of the period, or non-uniformly sampled radiocarbon data (i.e. neither the latest EB I nor the earliest EB II has been dated at all the sites). However, at the sites with the most robust data this transition took place c. 3100–3000 BC. On the other hand, the EB II to EB III transition is very well defined, yielding a transition date around 2900 BC (appearing in Fig. 1 as an almost horizontal line).

Construction and Abandonment of the EB Ib Great Temple

The results of this study allow us to be more precise in our dating of the EB Ib Great Temple, which previous typological and radiocarbon studies suggested was ca. 3000 BC (Boaretto 2006; Adams 2013a; Adams, Finkelstein, and Ussishkin 2014). Sample RTK-6742 was taken from the constructional matrix of the Level J-4 temple, providing a *terminus post quem* for the construction of the edifice at 3090–2930 BC (1σ range). Further, Sample RTK-6732, found within the collapsed debris of the structure (Level J-4a), provides a *terminus ante quem* for its abandonment at 3020–2920 BC. That is, the Great Temple was constructed, occupied, and abandoned within the maximum span of 3090–2920 BC.

It is of note that the new Egyptian radiocarbon chronology places the accession of the Egyptian king Aha at c. 3111–3045 BC (68%; Dee *et al*. 2013). The range gives a significant probability to the fact that the construction of the Great Temple post-dated the reign of Aha's predecessor, Narmer. The significance of the observation is that it is during the reign of the latter that Egypt maintained a brief cultural, economic, and political presence on the southern coast of the Southern Levant (de Miroschedji 2002; Yekutieli 2007 and references therein). The new radiocarbon chronologies from Egypt and the Levant, then, provide the most precise data with which to conclude that the Egyptian "colonies" on the southern coast came and went immediately preceding the monumental leap in construction activity represented by the Great Temple (Adams, Finkelstein, and Ussishkin 2014). While not conclusive, it may be that there was a cause and effect relationship between these two phenomena.

The dates relating to the abandonment of the Great Temple seem to demonstrate that the EB I at Megiddo may have continued into the 30th Century BC (3000–2900 BC). According to the new ^{14}C results for the Early Bronze Age (Regev *et al*. 2012), this late date already sees the rise of EB II culture at other sites. While it is possible that ceramic definitions of EB II vs. late EB I are problematic, especially with regard to samples from

old excavations (Regev *et al*. 2012: 558), the evidence from Megiddo seems to support an alternative hypothesis, that the beginning of the EB II at some sites is contemporary with the end-phase of the EB Ib at others. In addition to the radiocarbon data presented here, new excavations at Tel Megiddo East (the settlement responsible for the construction of the Great Temple at Megiddo; Adams *et al*. 2014) have revealed that the final phases of the EB Ib (contemporary with Level J-4) are defined by classic late EB I material culture with the addition of Northern Canaan Metallic Ware (NCMW), a hallmark of the EB II (Greenberg and Porat 1996). The latter was apparently imported from the Hula or Upper Jordan Valleys, where EB II ceramic culture was already present and apparently defining an emerging territorial entity (Greenberg 2003). The chronological synchronisms made possible with the new radiocarbon dates suggest the possibility that the collapse of EB Ib Megiddo, as a vital center in the western Jezreel Valley, was connected to the rise of an EB II territorial entity in the Jordan Valley, possibly centered at Tel Bet Yerah.

Short duration of EB II

The stratigraphic analysis of Megiddo indicates that the site had been abandoned for some time (Level J-4a), before it was rebuilt in the EB III as Level J-5. Based on the models for the Megiddo data (Figs. 7–9), the duration of the occupational gap between the end of EB IB (Level J-4) and the early phase of the EB III (Level J-5), is estimated by the model to be 0–180 years. Interestingly, when looking at the curve plot (Fig. 8), no modeled dates from Megiddo fall on the narrow slope between 2920–2820 BC. In other sites, the last part of the 30th century BC corresponds to the last phase of EB II, while at Megiddo no EB II occupation took place in Area J. The EB IB to EB II transition at Megiddo could have occurred as early as c. 3000 BC, but without additional radiocarbon data for Level J-4a, the precise length of the period of abandonment remains unknown.

Subdivision and transitions within the EB III phases

The wiggle matching of short-lived samples applied here, offers precise dates for the three EB III phases at Megiddo: Level J-5 between 2850–2800 BC, Level J-6b between 2800–2700 BC and Level J-6a between 2750/2700–2600/2500 BC (Table 4). Such time precision is attained for a period with "wiggly" calibration curve due to the dense sampling of clear superimposed stratigraphy well connected to high quality contexts. Since this type of sampling and modeling depends first upon correct archaeological assignment, tightly controlled archaeological conditions are essential. Thus, the necessity of our microstratigraphical approach to context characterization from where the radiocarbon samples were collected.

Similar modeling, but on a stratigraphy constructed across an archaeological site rather than on directly superimposed stratigraphy (as here), was performed at Tel Yarmuth (Regev, de Miroschedji, and Boaretto 2012), but there the earliest EB III phase was not measured as no material for dating was recovered. For the rest of the EB III sub-phases there is a good agreement between the transitions modeled in the two sites, perhaps suggesting cross-regional developments. However, in the case of Tel Yarmuth, wiggle-matching of the samples along the calibration curve was not possible.

End of EB III

The new radiocarbon-based chronology for the Early Bronze put forth by Regev *et al.* (2012) showed that the EB III ended around 2500 BC, 200–300 years earlier than traditionally thought. Samples extracted from EB III occupation layers at Bet Yerah, Hebron, Tell-el-Hesi, Numeira, Tell el-Umeiri, Tel Yarmuth, Khirbet es-Zeraqun (Regev *et al*. 2012) and Tell es-Safi (Shay *et al*. 2014) all support this conclusion. The results from Megiddo fit well this emerging pattern, showing that Level J-6a ended ca. 2600/2500 BC.

There is disagreement whether or not Level J-6a represents the last phase of the EB III at Megiddo. Though the original excavators attributed the succeeding Level J-7 (OI Stratum XV) to the Intermediate Bronze Age (their "MB I"; Loud 1948; 78–84), later scholars argued for a late EB III date for this layer (e. g. Dunayesky and Kempinski 1973; Esse 1991 and references). The problem has not been resolved as evidenced by the ongoing discussion between Adams, who prefers to see Level J-7 belonging to the Intermediate Bronze Age (Adams 2013a, b; forthcoming) and Finkelstein, who supports an EB III date (Finkelstein 2013). Unfortunately, no J-7 accumulation is currently accessible for further excavations and

hence no radiocarbon samples are available for this phase. Therefore, the problem cannot currently be determined radiometrically. As long as this issue remains unresolved, we cannot say whether or not the Level J-6a end-date of 2600/2500 BC (the latest possible dates according to ±1σ range could fall as late as ca. 2500 BC – see Fig. 8) represents the end of the EB III at the site. One way or the other, there is "room" within the radiocarbon model for Level J-7 to fit within the new radiocarbon chronologies' EB III end-date of 2500 BC, but the data also does not force it into this position.

Synchronizing the EB III of the Southern Levant with Egyptian Chronology

Fixing the collapse of the Southern Levantine EB III urban system at ca. 2500 BC forces a reconsideration of the synchronism between Egypt and the Southern Levant that has far-reaching implications for the history and chronology of both regions. According to the traditional chronology (Fig. 1), the EB III with dates of ca. 2700–2300/2200 BC (e. g., Mazar 1992; Ben-Tor 1992), overlapped with the Egyptian 3rd to 6th Dynasties (the Old Kingdom), and the demise of the EB III urban civilization in the Southern Levant was roughly contemporary with or slightly predated the decline of the Old Kingdom and the 6th Dynasty (e. g. Sowada 2009: 4); thus the collapses of the two cultures has been seen as interrelated (e. g. Ben-Tor 1992).

According to radiocarbon determinations for Predynastic through Old Kingdom finds (Fig. 1; Bronk Ramsey *et al*. 2010; Dee *et al*. 2013) and the new radiocarbon-based chronology of the Early Bronze Southern Levant (Regev *et al*. 2012), the EB III (c. 2900–2500 BC) spans from the very late 1st Dynasty (Naqada IIIC2) to the middle/late 4th Dynasty (ca. reigns of Khafre/Shepseskaf). Further, the Intermediate Bronze Age in the Southern Levant corresponds with the Egyptian late 4th Dynasty through the rest of the Old Kingdom and First Intermediate Period (Fig. 1).

The traditional correlation between the EB III and the Old Kingdom rests on three arguments:

1. The presence of EB III ceramics in Egyptian tombs of the Old Kingdom whose date according to the Egyptian historical chronologies could be well established on the basis of inscribed material and cemetery development (Stager 1992; Sowada 2009); imported EB III Levantine vessels in Egypt are typologically restricted to (a) two-handled combed flat-based jars and (b) one-handled non-combed jugs ("Abydos ware") found in tombs datable to the 4th through 6th Dynasties.[9]
2. Egyptian objects, such as mace-heads, palettes, stone vessels, and ivory objects, found in EB III contexts at numerous sites in the Southern Levant (see list in Sowada 2009: Table 5).
3. Egyptian Old Kingdom texts of the 5th and 6th Dynasties, which attest to foreign expeditions, assumed to have taken place in the Southern Levant (e. g. de Miroschedji 2002; Sowada 2009).

In light of the new radiocarbon data which precludes chronological overlap between the Southern Levantine EB III and the Egyptian 5th and 6th Dynasties, these arguments need to be reevaluated. While a thorough treatment is outside the scope of this paper, the following comments are in place:

A. It has long been recognized that the two types of vessels found in Egyptian tombs dating to the Old Kingdom are part of the general repertoire of both the Northern and Southern Levant in the EB II/III, but the precise point of origin has been difficult to trace (Esse 1991: 109). Metrical, petrographic and chemical evidence (Esse 1991: 109–116; Porat 1989 and Greenberg and Porat 1996; Esse and Hopke 1986 and Sowada 2009 respectively) demonstrate that these types arrived in Egypt from the northern Levant (Knoblauch 2010),[10] where EB III/IV material ceramic culture does, in fact, continue until ca. 2200/2000 BCE (Akkermans and Schwartz 2003).

B. Nearly all of the Egyptian artifacts found in EB III contexts have been shown to date typologically to the Naqada III period through the 3rd/4th Dynasties (see Sowada 2009: Table 5). On the assumption that the EB III must correspond to the 5th/6th Dynasties, these objects have been interpreted as heirlooms (Sowada 2009: 125, 230–232). Given the new radiocarbon chronology, it is clear that they reflect real-time exchange.

[9] See discussion and catalog in Sowada 2009: 54–90, Table 4; 154–182. The later type (b) does not appear in 6th Dynasty contexts (Knoblauch 2012: 255).

[10] Despite these data, scholars have maintained – with no evidence – that some of the vessels must also be the result of trade with the southern Levant (Esse and Hopke 1986; Kantor 1992; de Miroschedji 2002).

C. Locations from the Sinai to the northern Levant have been proposed as the targets of the Egyptian razzias into the Levant evident in 5th and 6th Dynasty texts (e. g. Weni, Pepynakht, etc.; see overview in Sowada 2009: 10–15). In fact, the localities and groups mentioned with respect to them are unidentifiable. Whether they reflect other towns in Egypt, towns in the northern Levant, or idealized conquests, it is now certain that they cannot represent contemporary Southern Levantine towns.

Egypt and Levantine Interactions of the 3rd millennium BC – A Revised Outline

The implications of this revised understanding of the synchronism between Egypt and the Levant are numerous, and they call for revision in our historical and archaeological understanding of the 3rd Millennium BC. As the basis for future study, the following outline of Egyptian-Levantine chronological synchronisms may be put forth.

In the EB IB, the incipient Egyptian state (Naqada IIIC1; early 1st Dynasty) established settlements in the southern coastal plain of the Levant and interacted directly with the local inhabitants (de Miroschedji 2002; Yekutieli 2007 and references). In reaction, regions immediately outside of the general Egyptian influence, i.e. the Jezreel and Jordan Valleys, underwent proto-urban developments (e. g. the relatively prosperous period of Level J-3 Megiddo; see also Greenberg and Eisenberg 2002). Leading up to the transition to the EB II, and following the reign of the Egyptian king, Narmer (ca. 3050–2950 BC), the Egyptian settlements were abandoned in favor of a more distanced but targeted strategy of interaction. It may be that this abandonment and new strategy provided a political and/or economic boost to certain regions such as Megiddo, which allowed for the construction of the Great Temple. The brief EB II period, broadly speaking 3000–2900 BC, coincided with the remainder of the Egyptian 1st Dynasty (Naqada IIIC2), and appears to be a period of power and settlement reorganization in the Southern Levant, possibly as a result of the Egyptian abandonment or, less likely, causing it. EB II territorial entities emerged in the upper Jordan Valley (possibly contributing to the collapse of Megiddo) and in the south in the Arad Valley, both of which enjoyed commercial relationships with Egypt in the 1st Dynasty (Adams and Porat 1996; Amiran and Ilan 1992; Greenberg and Eisenberg 2002).

The ultimate result of the EB II reorganization was the emergence of the EB III urban and territorial system, based on fortified central cities endowed with palaces (e. g. Megiddo, Yarmuth, Ai) dating from ca. 2900–2500 BCE and spanning from the late 1st Dynasty (Naqada IIIC2/D) to the early/middle of the 4th Dynasty (ca. reigns of Khafre/Shepseskaf). During this time, the interaction between the Egyptian kings and Levantine urban territorial entities resulted in the acquisition by the latter of Egyptian prestige objects, such as stone vessels, mace heads, and palettes.

Toward the end of the Southern Levantine EB III, the Egyptian state reached the apex of its hierarchical development, with its ability to mobilize a tremendous workforce for the construction of massive pyramids. Conversely, the cohesion of the urban territorial entities in the Southern Levant corroded. At the same time, Egyptian interactions with Byblos and the northern Levant intensified; inscribed material therein from the reign of Snefru/Khufu signifies the escalation of this connection. The Byblian/Egyptian interaction is also documented by evidence for the receipt of large quantities of wood (*Cedrus libani*), oil, and the combed Metallic Ware pottery discussed above. By ca. 2500, the collapse of the Southern Levantine EB III was complete and the region entered a period that is decidedly non-urban (Intermediate Bronze Age). The EB III of the northern Levant, however, remained highly organized and Byblos, in particular, continued its lucrative relationship with the Egyptian kings of the 4th – 6th Dynasties. Whether the shift in Egyptian interest from the south to the north was a cause or a result of the collapse of the southern EB III is difficult to ascertain at this time.

Summary

The microstratigraphic excavation of the EB at Megiddo produced a group of radiocarbon samples from the EB I and EB III periods which could be dated and then wiggle matched according to the calibration curve to produce a high-resolution chronology of the period. Overall, the results from Megiddo support the new dating of the EB developed from other sites in the Southern Levant. What both studies have highlighted is that there is much need for an audit of the synchronisms between Egyptian and Levantine chronologies and a revision of our understanding of the interrelations between the two regions for the 3rd Millenni-

um. On this front, it can now be said that the Southern Levantine EB III comes to an end in the era of the 4th Dynasty. This absolute chronological synchronism provides new explanations for the presence of Egyptian artifacts in the Levant during the EB III and of the Levantine pottery in Egyptian tombs. Based on these observations, a new outline of Egyptian/Levantine interactions was put forth to lay the groundwork for a reappraisal of the voluminous data on the subject.

Bibliography

Adams, M.J.

2013a Area J (The 2004–2008 Seasons). Part III: The Early Bronze Age, Stratigraphy and Architecture, 47–118, in: I. Finkelstein, D. Ussishkin, E. Cline, M. Adams, E. Arie, N. Franklin, and M. Martin (eds.), *Megiddo V: The 2004–2008 Seasons*, Sonia and Marco Nadler Institute of Archaeology Monograph Series 31, Tel Aviv.

2013b The Early Bronze Pottery from Area J, 295–334, in: I. Finkelstein, D. Ussishkin, E. Cline, M. Adams, E. Arie, N. Franklin, and M. Martin (eds.), *Megiddo V: The 2004–2008 Seasons*, Sonia and Marco Nadler Institute of Archaeology Monograph Series 31, Tel Aviv.

Forthcoming The Egyptianizing Pottery from Megiddo Area J, Revisited. Stratigraphy, Form, Function and Implications for the Three Temples in Antis.

Adams, M.J., David, J., Homsher, R., Cohen, M.E.

2014 New Evidence for the Rise of a Complex Society in the Late Fourth Millennium at Tel Megiddo East in the Jezreel Valley, *Near Eastern Archaeology* 77:1: 32–43..

Adams, M.J., Finkelstein, I., and Ussishkin, D.

2014 The Great Temple of Early Bronze I Megiddo, *AJA* 118.2: 1–21.

Adams, B., and Porat, N.

1996 Imported Pottery with Potmarks from Abydos, 98–107, in: J. Spencer (ed.), *Aspects of Early Egypt*, London.

Akkermans, P.M.M.G., and Schwartz, G.M.

2003 *The Archaeology of Syria. From Complex Hunter-Gatherers to Early Urban Societies (ca. 16,000–200 BC)*, Cambridge.

Amiran, R., and Ilan, O.

1992 *Arad: Eine 5000 Jahre alte Stadt in der Wüste Negev, Israel*, Neomünster.

Berna, F., Behar, A., Shahack-Gross, R., Berg, J., Boaretto, E., Gilboa, A., Sharon, I., Shalev, S., Shilshtein, S., Yahalom-Mack, N., Zorn, J.R., and Weiner, S.

2007 Sediments Exposed to High Temperatures: Reconstructing Pyrotechnological Processes in Late Bronze and Iron Age Strata at Tel Dor (Israel), *Journal of Archaeological Science* 34: 358–373.

Boaretto, E.

2006 Radiocarbon Dates, 550–557, in: I. Finkelstein, D. Ussishkin and B. Halpern (eds.), *Megiddo IV: The 1998–2002 Seasons*, Sonia and Marco Nadler Institute of Archaeology Monograph Series 24, Tel Aviv.

Bronk Ramsey, C.

2009 Bayesian analysis of radiocarbon dates, *Radiocarbon* 51(1): 337–360.

Bronk Ramsey, C., Dee, M.W., Rowland, J.M., Higham, T.F.G., Harris, S.A., Brock, F., Quiles, A., Wild, , E.M., Marcus, E.S., Shortland, A.J.

2010 Radiocarbon-Based Chronology for Dynastic Egypt, *Science* 328: 1554–1557.

Carmi, I., and Segal, D.

2000 Radiocarbon dates, 502–503, in: I. Finkelstein, D. Ussishkin, and B. Halpern (eds.), *Megiddo III: The 1992–1996 Seasons*, Sonia and Marco Nadler Institute of Archaeology Monograph Series 18, Tel Aviv.

Chu, V., Regev, L., Weiner, S., and Boaretto, E.

2008 Differentiating between Anthropogenic calcite in Plaster, Ash and Natural Calcite Using Infrared Spectroscopy: Implications in Archaeology, *Journal of Archaeological Science* 35, 905–911.

Dee, M., Wengrow, D., Shortland, A., Stevenson, A., Brock, F., Flink, L.G., and Bronk Ramsey, C.

2013 An Absolute Chronology of Early Egypt Using Radiocarbon Dating and Bayesian Statistical Modeling, *Proceedings of Royal Society A: Mathematical, Physical and Engineering Sciences* 469, 1–10.

Dunayevsky, I., and Kempinski, A.

1973 The Megiddo Temples, *Zeitschrift des Deutschen Palästina-Vereins* 89: 161–187.

Esse, D.

1991 *Subsistence, Trade and Social Change in the Early Bronze Age Palestine*, Studies in Ancient Oriental Civilization 50, Chicago.

Esse, D., and Hopke, P.

1986 Levantine Trade in the Early Bronze Age, 327–339, in: J.S. Olin and J. Blackman (eds.), *Proceedings of the 24th International Archaeometry Symposium*, Washington.

Finkelstein, I.

2013 Archaeological and Historical Conclusions, 1329–1340, in: I. Finkelstein, D. Ussishkin, E. Cline, M. Adams, E. Arie, N. Franklin, and M. Martin (eds.), *Megiddo V: The 2004–2008 Seasons*, Sonia and Marco Nadler Institute of Archaeology Monograph Series 31, Tel Aviv.

Finkelstein, I., and Ussishkin, D.

2000 Area J, 25–74, in: I. Finkelstein, D. Ussishkin, and B. Halpern (eds.), *Megiddo III: The 1992–1996 Seasons*, Sonia and Marco Nadler Institute of Archaeology Monograph Series 18, Tel Aviv.

Finkelstein, I., Ussishkin, D., and Peersmann, J.

2006 Area J (The 1998–2000 Seasons), 29–53, in: I. Finkelstein, D. Ussishkin, and B. Halpern (eds.), *Megiddo IV: The 1998–2002 Seasons*, Sonia and Marco Nadler Institute of Archaeology Monograph Series 24, Tel Aviv.

Friesem, D. and Shahack-Gross, R.

2013 Area J, Part V: Analyses of Sediment from the Level J-4 Temple Floor, 295–334, in: I. Finkelstein, D. Ussishkin, E. Cline, M. Adams, E. Arie, N. Franklin, and M. Martin (eds.), *Megiddo V: The 2004–2008 Seasons*, Sonia and Marco Nadler Institute of Archaeology Monograph Series 31, Tel Aviv.

Greenberg, R.

2003 Early Bronze Age Megiddo and Bet Shean: Discontinuous Settlement in Sociopolitical Context, *Journal of Mediterranean Archaeology* 16.1, 17–32.

Greenberg, R., and Eisenberg, E.

2002 Egypt, Bet Yerah, and Early Canaanite Urbanization, 213–222, in: E.C.M. van den Brink and T.E. Levy (eds.), *Egyptian-Canaanite Interaction: From the 4th through Early 3rd Millennium B.C.E.*, New Approaches to Anthropological Archaeology, London.

Greenberg, R., and Porat, N.

1996 A Third Millennium Levantine Pottery Production Center: The Typology, Petrography, and Provenance of the Metallic Ware of Northern Israel and Adjacent Regions, *BASOR* 301, 5–24.

Hornung, E., Krauss, R., Warburton, D.A.

2006 *Ancient Egyptian Chronology*, HdO 83, Leiden.

Kantor, H.

1992 The Relative Chronology of Egypt and its Foreign Correlations before the First Intermediate Period, 3–21, in: R. Ehrich (ed.), *Chronologies in Old World Archaeology*, 3rd ed., Chicago.

Kitchen, K.

1991 The Chronology of Ancient Egypt, *World Archaeology* 23(2): 201–208.

Knoblauch, C.

2010 Preliminary Report on the Early Bronze Age III Pottery from Contexts of the 6th Dynasty in the Abydos Middle Cemetery, *Ägypten und Levante* 20 243–261.

Loud, G.

1948 *Megiddo II: Seasons of 1935–39*. Chicago.

Mazar, A.

1992 *Archaeology of the Land of the Bible, 10,000–586 B.C.E*, New York.

de Miroschedji, P.

2002 The Socio-political Dynamics of Egyptian-Canaanite Interaction in the Early Bronze Age, 39–57, in: E.C.M. van den Brink and T.E. Levy (eds.), *Egyptian-Canaanite Interaction: From the 4th through Early 3rd Millennium B.C.E.*, New Approaches to Anthropological Archaeology, London.

Porat, N.

1989 *Composition of Pottery. Application to the Study of the Interrelations between Canaan and Egypt during the 3rd Millennium BC*, Unpublished PhD Thesis, Hebrew University of Jerusalem, Jerusalem.

Rebollo, N.R., Cohen-Ofri, I., Popovitz-Biro, R., Bar-Yosef, O., Meignen, L., Goldberg, P., Weiner, S., and Boaretto, E.

2008 Structural Characterization of Charcoal Exposed to High and Low pH: Implications for ^{14}C Sample Preparation and Charcoal Preservation, *Radiocarbon* 50(2): 289–307.

Reimer, P.J., Baillie, M.G.L., Bard, E., Bayliss, A., Beck, J.W., Blackwell, P.G., Bronk Ramsey, C., Buck, C.E., Burr, G.S., Edwards, R.L., Friedrich, M., Grootes, P.M., Guilderson, T.P., Hajdas, I., Heaton, T.J., Hogg, A.G., Hughen, K.A., Kaiser, K.F., Kromer, B., McCormac, F.G., Manning, S.W., Reimer, R.W., Richards, D.A., Southon, J.R., Talamo, S., Turney, C.S.M., van der Plicht, J., Weyhenmeyer, C.E.

2009 IntCal09 and Marine09 Radiocarbon Age Calibration Curves, 0–50,000 cal BP., *Radiocarbon* 51(4): 1111–1150.

Regev, J., de Miroschedji, P., and Boaretto, E.

2012 Early Bronze Age Chronology: Radiocarbon Dates and Chronological Models from Tel Yarmuth (Israel), *Radiocarbon* 54(3–4), 505–524.

Regev, J., de Miroscedji, P., Greenberg, R., Braun, E., Greenhut, Z., and Boaretto, E.

2012 Chronology of the Early Bronze Age in the South Levant: New Analysis for a High Chronology, *Radiocarbon* 54(3–4), 525–566.

Regev, L., Poduska, K.M., Addadi, L., Weiner, S., and Boaretto, E.

2010 Distinguishing between Calcites Formed by Different Mechanisms Using Infrared Spectrometry: Archaeological Applications, *Journal of Archaeological Science* 37, 3022–3029.

Shai, I., Greenfield, H. J. , Regev, J., Boaretto, E., and Maeir, A.

2014 The Early Bronze Age Remains at Tell es-Safi/Gath, Israel: An Interim Report, *Tel Aviv* 41(1), 20–49.

Sowada, K.N.

2009 *Egypt in the Eastern Mediterranean during the Old Kingdom*, OBO 237, Fribourg.

Stager, L.

1992 The Periodization of Palestine from Neolithic through Early Bronze Times, 22–41, in: R. Ehrich (ed.), *Chronologies in Old World Archaeology*, 3rd ed., Chicago.

Stuiver, M., and Polach, H.A.

1977 Discussing Reporting ^{14}C Data, *Radiocarbon* 19(3): 355–363.

Ussishkin, D.

2013 Comments regarding The Early Bronze Cultic Compound, 1992–2010, 1317–1328, in: I. Finkelstein, D. Ussishkin, E. Cline, M. Adams, E. Arie, N. Franklin, and M. Martin (eds.), *Megiddo V: The 2004–2008 Seasons*, Sonia and Marco Nadler Institute of Archaeology Monograph Series 31, Tel Aviv.

Yekutieli, Y.

2007 The Relations between Egypt and Canaan in the Early Bronze Age 1 – A View from Southwestern Canaan, [in Hebrew] *Qadmoniot* 134, 66–74.

Yizhaq, M., Mintz, G., Cohen, I., Khalally, H., Weiner, S., and Boaretto, E.

2005 Quality controlled radiocarbon dating of bones and charcoal from the early Pre-Pottery Neolithic B (PPNB) of Motza (Israel), *Radiocarbon* 47: 193–206.

Weiner, S.

2010 *Microarchaeology – Beyond the Visible Archaeological Record*, Cambridge.